RESIDUAL IMAGE CODING USING TRELLIS QUANTIZATION

Tomas Eriksson, Norbert Goertz*

Inst. for Digital Communications
The University of Edinburgh
Edinburgh EH9 3JL, UK

Mirek Novak

Dept. of Information Technology
Lund University, Box 118
SE-221 00 Lund, Sweden

ABSTRACT

We consider the lossy image compression problem and propose a model-residual approach. Polynomial basis images encode the model image and powerful new trellis codes quantize the residual part. A simple bit allocation scheme determines the residual bit rates. Results are shown for the 0.4–1.6 bits per pixel region. Comparisons are made to several state-of-the-art techniques and show that the proposed scheme is very competitive.

1. INTRODUCTION

Digital image communication has become increasingly popular during the past years. Uncompressed digital images require a very high storage (or transmission) capacity. Thus it is of vital importance to find suitable methods for data reduction in the context of image communication. Modern image coding is often based on transforms in one form or another. The purpose of applying the transform is to find a representation suitable for compression (lossy or lossless). While most state-of-the-art methods are based on the increasingly popular wavelet transform (see, e.g., [1], [2], [3], [4], [5]), a different path has been chosen in this paper.

We propose an image compression system based on a model-residual representation. Polynomial basis images are used to represent the model components and the corresponding quantization error, i.e., the residual image signal, is encoded by a trellis quantizer based on a class of the newly proposed SR/LC codes [6]. The rate allocation of the residual encoder is given by a simple classification scheme which also provides the possibility of progressive transmission. Simulation results are given for a number of different bit rates and test images. The paper is concluded with a comparison to state-of-the-art methods and a discussion on the perceptual quality of the encoded images. It should be mentioned that in this work we only consider monochrome, or grayscale, images. However, the proposed method is easily adapted to color images. It should also be mentioned that only photographic pictures of natural elements are suitable for the lossy compression methods presented here.

2. MODEL-RESIDUAL REPRESENTATION OF IMAGES

The model-residual concept takes advantage of the fact that many real-life signals, such as speech and photographic images, can be characterized by a combination of long-term and short-term descriptions, respectively. The original source signal is thus divided into two parts and we refer to these as the *model* and the *residual* signals, respectively. These parts are processed independently with different methods. There are two main advantages with quantizing one small part of the image, a so-called *subimage*, at a time. First, the computational burden can be significantly reduced. Second, local pixel variations can be captured by a small-block encoder. Blocking artifacts can be reduced with the appropriate quantization method.

A set of basis images $\boldsymbol{b}_w$, $w = 0, 1, \ldots, W-1$ serves as the model. The model basis images are defined as matrices of the same dimension as the subimages, namely $N_1' \times N_2'$ pixels. The model subimage is then represented by a weighted sum of basis images. We consider only orthonormal basis images and hence the model images can be written as

$$\boldsymbol{m}_s = \sum_{w=0}^{W-1} p_s^{(w)} \cdot \boldsymbol{b}_w, \tag{1}$$

where $p_s^{(w)}$ is the wth model coefficient, or weighting factor, for subimage s. W is the number of basis images used in the model. The wth model coefficient for the original subimage block $\boldsymbol{x}_s$ is

$$p_s^{(w)} = \sum_{n_1=1}^{N_1'} \left(\sum_{n_2=1}^{N_2'} x_s[n_1, n_2] \cdot b_w[n_1, n_2] \right), \tag{2}$$

where $x_s[n_1, n_2]$ is the picture element at position $[n_1, n_2]$ in subimage s. Thus $p_s^{(w)}$ describes how much of $\boldsymbol{x}_s$ that is spanned by the hyperplane defined by $\boldsymbol{b}_w$. From (1) and (2) it follows that the residual image block $\boldsymbol{r}_s$ can be written as

$$\begin{aligned} \boldsymbol{r}_s &= \boldsymbol{x}_s - \boldsymbol{m}_s = \boldsymbol{x}_s - \sum_{w=0}^{W-1} p_s^{(w)} \cdot \boldsymbol{b}_w \qquad (3) \\ &= \boldsymbol{x}_s - \sum_{w=0}^{W-1} \left(\sum_{n_1=1}^{N_1'} \left(\sum_{n_2=1}^{N_2'} x_s[n_1, n_2] \cdot b_w[n_1, n_2] \right) \right) \cdot \boldsymbol{b}_w. \end{aligned}$$

The last equality holds only if the model coefficients are not quantized. A study on different types of basis images was performed in [7]. The results showed that the polynomial structure had the best performance of all types of basis images considered in the survey. Polynomial basis images, as used in the current work, were first proposed in [8].

The left-hand side of Figure 1 shows a segment of the model image of the test image `lena`. The corresponding residual image is shown in the right-hand part. In both figures blocking artifacts are clearly visible. In the following we will show how these effects can be significantly reduced. Since the model coefficients are real-valued they must be quantized before transmission or storage. However, it was shown in [7] that only $R_{\text{mod}} = 0.1$ bits per pixel (bpp) are

*This work was funded by EPSRC grant EP/D 002184/1. Contact author: `tomas.eriksson@ed.ac.uk`.

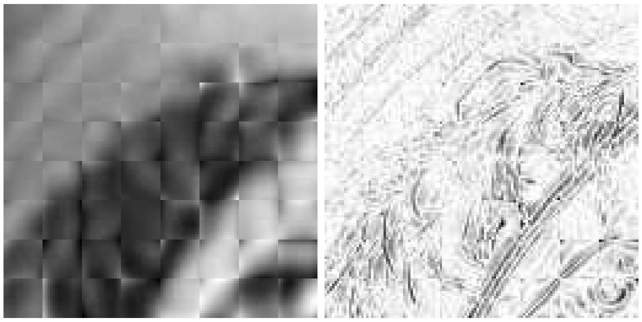

Fig. 1. Test image `lena`. Segment of model image (left), and residual image (right). Block size 16×16 and $W = 6$. In the right-hand side the grayscale has been inverted for better printability.

	W	4		6		10	
Image	N'	8	16	8	16	8	16
`lena`		29.18	25.83	31.73	27.18	33.78	28.33
`goldhill`		28.62	25.71	30.29	26.72	31.80	27.68

Table 1. Model PSNR in dB for the test images as a function of W and subimage size. $N_1' = N_2' = N'$.

needed in order to represent a model subimage of size 8×8 pixels with $W = 6$. Table 1 summarizes the model PSNR for different test images.

3. ENCODING OF THE RESIDUAL SUBIMAGES

Since the model removes low frequency components, the residual image has elements that are noise-like. Hence a candidate method for quantizing the residual components is trellis based quantization. The actual trellis codes will be further discussed below. Before quantization the residual blocks are serialized according to the Peano–Hilbert (PH) method. It should be mentioned that only quantization of blocks with the same size as the model subimages is considered. Unfortunately the residual blocks are non-stationary and thus it cannot be assumed that they have variance one. Therefore all residual blocks are normalized before quantization. All residual blocks have mean zero since the first model component corresponds to the mean value of each block. The variance of each block can be transmitted at a very low additional rate per pixel.

3.1. Trellis Quantizer Parameters

A number of parameters must be specified for the trellis quantizers. These include the actual choice of codes, reproducer alphabets, quantization rate estimations, and encoder algorithm. The trellis quantizers utilized in the current work are based on the newly developed SR/LC trellis codes. Details are given in [6]. These have been shown to have very competitive performance. The SR/LC trellis codes deploy the usual forward shift register (SR) state-transitions. The label on the kth branch stemming from state i, $i = 0, 1, \ldots, M-1$, is generated according to

$$l_i^{(k)} = (g^{(k)} \cdot i + a^{(k)}) \bmod M, \quad k \in \{0, 1, \ldots, 2^R - 1\}, \quad (4)$$

where $R \geq 1$ is the (integer) source coding rate of the trellis quantizer. $g^{(k)}$ and $a^{(k)}$ are design parameters. Good design parameters are listed in [9]. SR/LC trellis codes are easily extended to fractional rates by having multiple labels per branch.

Each of the M labels is mapped to a reproducer value and we simply associate the jth label with the jth reproducer value. Since it is assumed that the PDF of the residuals is close to either that of the Gaussian or Laplacian, the initial reproducer value sets were chosen to match these distributions. Thus

$$y_j = F^{-1}\left(\frac{2j+1}{2M}\right), \quad j = 0, 1, \ldots, M-1, \quad (5)$$

where $F(x)$ is either the Gaussian or Laplacian CDF. For the present application the codes with Gaussian reproducer letters performed on average 0.5 dB better for all test images, see Table 2. A more sophisticated approach is to utilize optimized alphabets. To generate these alphabets the procedure in [10] was used. For the optimization procedure a training set consisting of the residuals of a number of standard test images was used. To avoid biased codebooks each target image was removed from the training set.

It is often desired to include a lossless encoder in the trellis structure. A good estimate of the source coding rate in this case is the expectation of $-\log_2 \Pr\{y_j|\text{state } i\}$ averaged over all M states [11]

$$\bar{R} = -\sum_{i=0}^{M-1} \Pr\{\text{state } i\} \sum_{j=0}^{M-1} \Pr\{y_j|\text{state } i\} \log_2 \Pr\{y_j|\text{state } i\}, \quad (6)$$

where all quantities are estimated by simulations of the system.

Since the serialized residual blocks have relatively short block lengths, a candidate encoding algorithm is the tailbiting BCJR algorithm [12]. With some modifications to handle short blocks the standard Viterbi algorithm could also serve as an encoder.

3.2. Bit Allocation

Since the images are non-stationary the value of the PSNR will change from block to block. Hence it is desirable to allocate a higher residual bit rate to blocks with a low model PSNR. To solve this problem we propose a method in which the quantization rate is controlled by a threshold parameter θ. This procedure is similar to the subband classification process present in many wavelet based image coders, see e.g., [4], [5]. In our approach, the PSNR for each subimage of the model image is first computed. If the model PSNR is larger than θ a quantization rate of R_1 bits is used, else the residual is quantized with $R_2 > R_1$ bits. If $0 \leq \nu \leq 1$ is the fraction of subimages with a PSNR higher than the threshold, the residual bit rate is

$$R_{\text{res}} = (1-\nu) \cdot R_1 + \nu \cdot R_2. \quad (7)$$

With this method the value of θ determines the residual bit rate in the range $R_1 \leq R_{\text{res}} \leq R_2$. It also makes progressive transmission possible: as the rate (controlled by θ) increases, a higher number of residual blocks are encoded and transmitted. The total overhead for the bit allocation is just $1/N_1'N_2'$ bpp. It is possible that the components of R_1 and R_2 have been estimated by (6). However, note that this method by itself does not require entropy coding to produce a wide range of rates.

4. RESULTS

Table 2 shows PSNR scores for different test images using the model-residual approach. For the total bit rate $R_{\text{tot}} = R_{\text{mod}} + R_{\text{res}}$ lossless compression is not considered in this case. Moreover, the results in the table correspond to having $\theta = 0$, $R_1 = 1$, and $\nu = 0$ in (7).

Image	Gauss	Laplace	Optimized
`lena`	35.16	34.62	35.31
`goldhill`	34.02	33.53	34.18

Table 2. Model-residual approach. Encoded PSNR in dB using different sets of reproducer alphabets. Trellises have 8 states. $R_{\text{tot}} = 0.1 + 1.0$ bpp.

Thus all residual blocks are quantized with 1 bpp. The block size was set to 8×8 pixels and the model images all have $W = 4$. Thus the corresponding model PSNRs are given in the leftmost column of Table 1. In comparison to Table 1 the typical performance increase is about 5–6 dB for all images under consideration. These results are in accordance with pure rate-distortion quantization of IID memoryless sources.

Figure 2 shows the performance for codes with rate allocations according to (7) for different combination of R_1 and R_2. For the same bit rate the results in the figure are clearly better than those provided in Table 2. This shows the importance of proper bit allocation. The figure legends correspond to the settings listed in the associated table. Note that (a)–(c) utilize a perfect entropy coder for which the rates for the residual quantizers have been estimated according to (6) for each residual rate component. All the results are for trellises with 32 states and Gaussian reproducer values. By increasing the state-size from 8 to 32 states we improve the results for all test images by 0.3–0.4 dB in the $1 < R_{\text{tot}} < 1.6$ region. Again, these findings are consistent with usual trellis quantization of IID sources.

The main disadvantage with the proposed method is that no further gain in PSNR is possible after, say, 1.6–1.7 bpp. The reason is that the highest quantization rate used by the proposed method is $R = 2$ bits per sample for the residual part. Thus the maximum bit rate is $R_{\text{tot}} = 0.1 + 2.0 = 2.1$ bpp if the transmission of the model parameters is also take into account. However, this limitation is of no major importance if the image quality is high, i.e., around 40 dB, at this bit rate. For such a high PSNR a further increase in the PSNR will not yield a higher perceptual image quality for most practical applications.

With the PSNR plots at hand a comparison to methods proposed in the literature is possible. We only compare the PSNR-versus-rate performance and do not consider the computational complexities of the different methods. Such an analysis would be difficult to conduct on this limited space since the methods are based on different approaches. Table 3 compares the results of the proposed method (denoted “New”) to a number of state-of-the-art image coders. For this comparison the settings according to Figure 2 (c) were used. The entropy rate was estimated according to (6). Worth noticing is that all cited methods are based on the wavelet transform. Some of the methods in the table, viz. [2], [4], and [5], are also based on trellis quantization. Unfortunately no information regarding the trellis state sizes is given in any of the papers. For the results in Table 3 the new SR/LC trellis codes have 32 states. In conclusion, the new method performs within 2 dB from state-of-the-art for the test image `lena`. For the `goldhill` image the gap is even closer (within 1 dB). The same behavior has been observed at $R_{\text{tot}} = 0.5$ bpp.

We now turn our attention to the perceptual quality of the encoded images. Segments of the test images `lena` and `goldhill` encoded with $R_{\text{tot}} = 0.6$ bpp are shown in Figure 3. In comparison to the model image of `lena`, see Figure 1, the blocking artifacts have been significantly reduced. In this segment of the image only a

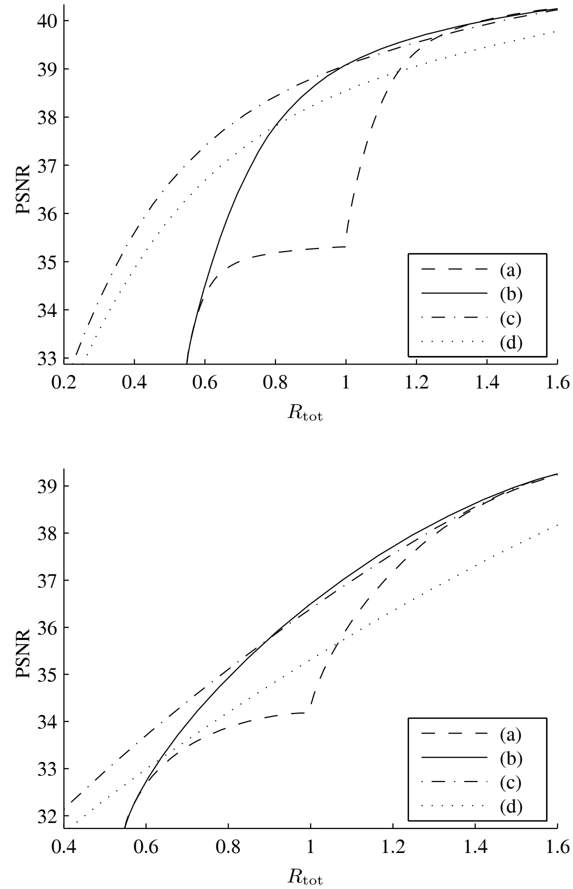

(a)	$R_1 = 1/2, R_2 = 1$ and $R_1 = 1, R_2 = 2$
(b)	$R_1 = 1/2, R_2 = 2$
(c)	$R_1 = 0, R_2 = 2$
(d)	Same as (c) but without entropy coder

Fig. 2. Model-residual approach. PSNR as a function of the total encoding rate. Test images `lena` (up) and `goldhill` (down).

Image	New	[1]	[2]	[3]	[4]	[5]
`lena`	39.1	39.6	39.9	40.5	41.1	41.2
`goldhill`	36.6	36.2	37.0	36.6	36.7	37.3

[1]	Shapiro: Embedded Zerotree Wavelet coder
[2]	Sriram and Marcellin: Entropy-Constrained TCQ
[3]	Said and Pearlman: Set Partitioning in Hierarchical Trees
[4]	Joshi *et al.*: Subband Classification
[5]	Xiong and Wu: Trellis Coded Space-Frequency Quantizer

Table 3. Comparison of proposed method to state-of-the-art image coders. $R_{\text{tot}} = 1.0$ bpp.

fraction of the blocks have been transmitted without residual encoding, see the hat band in the upper left quad of the figure. The reason is the large amount of details contained in this part of the original

Fig. 3. Magnified segments of the test images `lena` and `goldhill` encoded with 0.6 bpp.

Fig. 4. `lena` and `goldhill` encoded with 0.6 bpp. PSNR=37.4 dB and PSNR=33.7 dB, respectively.

image. In areas outside the face and the hat of the woman the situation is the reversed. A second example is given in the right-hand side of Figure 3 which shows a magnified part of the `goldhill` image. In this image the blocking artifacts are more apparent. However, one must remember that the images in Figure 3 show only a small segment (128×128 pixels) of the entire image (512×512 pixels). The full-sized encoded images are displayed in Figures 4. To the naked eye, the perceptual quality of the encoded images is almost indistinguishable to that of the original test images.

5. CONCLUSIONS AND FUTURE WORK

This paper has provided some applications that indicate that the newly developed SR/LC trellis codes can be useful in image coding. It is common knowledge that image compression should be based on invertible transforms only. Two examples frequently used in image coding are the discrete cosine transform and the discrete wavelet transform. However, the results in this paper show that a combination of a non-invertible transform, i.e., the model representation, and a powerful residual encoder, i.e., the trellis quantizer, could also be a successful approach. Since the energy of the residual components are not uniformly distributed over the whole residual image, a simple classification scheme was used to determine the bit rate for each block. This approach greatly increases the image quality at a negligible cost. Moreover, the classification scheme also makes possible a large range of encoding rates without the need of an entropy coder.

While the performance of the proposed method is quite promising, the main purpose of this paper has been to *introduce* the method as such and not to provide a fully optimized scheme. Thus future work considers further optimization of the system. Two possible topics include a more sophisticated bit allocation procedure and higher residual rates, cf. settings (a) and (c) in Figure 2. Another straightforward extension is to form a joint source and channel coding system based on the trellis structure.

6. REFERENCES

[1] J. M. Shapiro, "Embedded image coding using zerotrees of wavelet coefficients," *IEEE Trans. Signal Proc.*, vol. 41, no. 12, pp. 3445–3462, Dec. 1993.

[2] P. Sriram and M. W. Marcellin, "Image coding using wavelet transforms and entropy-constrained trellis-coded quantization," *IEEE Trans. Image Proc.*, vol. 4, no. 6, pp. 725–733, June 1995.

[3] A. Said and W. A. Pearlman, "A new, fast, and efficient image codec based on set partitioning in hierarchical trees," *IEEE Trans. Circ. Syst. for Video Techn.*, vol. 6, no. 3, pp. 243–250, June 1996.

[4] R. L. Joshi, H. Jafarkhani, J. H. Kasner, T. R Fischer, N Farvardin, M. W. Marcellin, and R. H. Bamberger, "Comparison of different methods of classification in subband coding of images," *IEEE Trans. Image Proc.*, vol. 6, no. 11, pp. 1473–1486, November 1997.

[5] Z. Xiong and X. Wu, "Wavelet image coding using trellis coded space-frequency quantization," *IEEE Signal Proc. Lett.*, vol. 6, no. 7, pp. 158–161, July 1999.

[6] J. B. Anderson and T. Eriksson, "Trellis source codes based on linear congruential recursions," *IEEE Comm. Lett.*, vol. 9, no. 3, pp. 198–200, Mar. 2005.

[7] M. Ahrholdt, "Lattice vector quantization of greyscale image residuals," M.S. thesis, Dept. Information Technology, Lund University, Sweden, 1998.

[8] R. Krishnamoorthi and P. Bhattacharyya, "A new data compression scheme using orthogonal polynomials," in *Proc. ICICS'97*, Singapore, Sep. 1997, vol. 1, pp. 490–494.

[9] T. Eriksson, *Trellis Source Coding Methods for Low Rates and Short Blocks*, Ph.D. thesis, Lund University, Sweden, 2005.

[10] L. C. Stewart, R. M. Gray, and Y. Linde, "The design of trellis waveform coders," *IEEE Trans. Comm.*, vol. COM-30, no. 4, pp. 702–710, April 1982.

[11] M. W. Marcellin, "On entropy-constrained trellis coded quantization," *IEEE Tran. Comm.*, vol. 42, no. 1, pp. 14–16, Jan. 1994.

[12] T. Eriksson, M. Novak, and J. B. Anderson, "MAP criterion trellis source coding for short sequences," in *Proc. DCC'03*, Snowbird, UT, Mar. 2003, pp. 43–52.